HHS Public Access

Author manuscript

J Thorac Oncol. Author manuscript; available in PMC 2020 May 01.

Published in final edited form as:

J Thorac Oncol. 2019 May ; 14(5): 802–815. doi:10.1016/j.jtho.2018.12.038.

Acquired *BRAF* rearrangements induce secondary resistance to EGFR therapy in *EGFR*-mutated lung cancers

Morana Vojnic[1], **Daisuke Kubota**[1], **Christopher Kurzatkowski**[1], **Michael Offin**[2], **Ken Suzawa**[1], **Ryma Benayed**[1], **Adam J. Schoenfeld**[2], **Andrew J. Plodkowski**[3], **John T. Poirier**[2,4], **Charles M. Rudin**[2,6], **Mark G. Kris**[2,6], **Neal X. Rosen**[2,5], **Helena A. Yu**[2,6], **Gregory J. Riely**[2,6], **Maria E. Arcila**[1], **Romel Somwar**[1,4], and **Marc Ladanyi**[1,4,*]

[1]Department of Pathology, Memorial Sloan Kettering Cancer Center

[2]Department of Medicine, Memorial Sloan Kettering Cancer Center

[3]Department of Radiology, Memorial Sloan Kettering Cancer Center

[4]Human Oncology and Pathogenesis Program, Memorial Sloan Kettering Cancer Center

[5]Molecular Pharmacology Program, Memorial Sloan Kettering Cancer Center

[6]Weill Cornell Medical College, Memorial Sloan Kettering Cancer Center

Abstract

Introduction: Multiple genetic mechanisms have been identified in *EGFR*-mutant lung cancers as mediators of acquired resistance (AR) to EGFR tyrosine kinase inhibitors (TKI) but many cases still lack a known mechanism.

*Address correspondence to: Marc Ladanyi, MD, ladanyim@mskcc.org.

CONFLICTS OF INTEREST STATEMENTS

Morana Vojnic, Daisuke Kubota, Christopher Kurzatkowski, Ken Suzawa, Michael Offin, Adam J. Schoenfeld, Andrew J. Plodkowski and J. T. Poirier have no relevant conflicts of interest to disclose.

Maria E. Arcila is a consultant for AstraZeneca and received support from Astrazeneca, Invivoscribe, and Raindance Technologies.

Alexander Drilon is a consultant for Ignyta, LOXO Oncology, TP Therapeutics, AstraZeneca, Pfizer, Blueprint Medicines, Genentech Roche, Takeda, and has received research funding from Foundation Medicine.

Helena A Yu is a consultant for AstraZeneca and received research funding from Astellas Pharma, Incyte, Lilly Oncology, Novartis, Daiichi, and AstraZeneca.

Charles M. Rudin is a consultant for Bristol-Myers Squibb, Abbvie, Seattle Genetics, Harpoon Therapeutics, Genentech Roche, and AstraZeneca.

Mark G. Kris is a consultant for Pfizer, Astrazeneca and Regeneron.

Neal X. Rosen has received research funding from Chugai, is on the Scientific Advisory Boards of Chugai, Astra-Zeneca, Beigene, Daichi-Sankyo and received consulting fees from Novartis, Boeringher-Ingelheim, Array, Revolutionary Medicines, and Tarveda. He has equity in Beigene, Kura, Z-Lab, Araxes and Fortress.

Gregory J. Riely received research funding from Novartis, Roche, Genentech, Millenium, GlaxoSmithKline, Pfizer, Infinity Pharmaceuticals and, ARIAD. He has received expense coverage from Merck Sharp & Dohme. He has a patent application submitted for pulsatile use of erlotinib to treat or prevent brain metastases.

Romel Somwar has received research support from Helsinn Healthcare.

Marc Ladanyi has received advisory board compensation from Boehringer Ingelheim, AstraZeneca, Bristol-Myers Squibb, Takeda, and Bayer, and research support from LOXO Oncology and Helsinn Healthcare.

Methods: To identify novel mechanisms of AR, we performed targeted large panel sequencing on 374 consecutive patients with metastatic *EGFR*-mutant lung cancer, including 174 post-TKI samples of which 38 patients also had a matched pre-TKI sample. Alterations hypothesized to confer AR were introduced into drug-sensitive *EGFR*-mutant lung cancer cell lines (H1975, HCC827, PC9) using CRISPR-Cas9 genome editing. MSK-LX138cl, a cell line with *EGFR* ex19del and *PJA2/BRAF* fusion, was generated from an EGFR TKI-resistant patient sample.

Results: We identified 4 patients (2.3%) with a *BRAF* fusion (3 *AGK/BRAF*, 1 *PJA2/BRAF*) in samples obtained at AR to EGFR TKI (2 post-erlotinib; 2 post-erlotinib and post-osimertinib). Pre-TKI samples were available in 2/4 patients and both were negative for *BRAF* fusion. Induction of *AGK/BRAF* fusion in H1975 (L858R+T790M), PC9 (ex19del) and HCC827 (ex19del) cells increased phosphorylation of BRAF, MEK1/2, ERK1/2 and STAT3, and conferred resistance to growth inhibition by osimertinib. MEK inhibition with trametinib synergized with osimertinib to block growth. Alternately, a pan-RAF inhibitor as a single agent blocked growth of all cell lines with mutant *EGFR* and *BRAF* fusion.

Conclusion: *BRAF* fusion is a mechanism of AR to EGFR TKI in approximately 2% of patients. Combined inhibition of EGFR and MEK (with osimertinib and trametinib) or BRAF (with a pan-RAF inhibitor) are potential therapeutic strategies that should be explored.

Keywords

Lung adenocarcinoma; *EGFR*; *BRAF* fusion; acquired resistance; osimertinib; CRISPR-Cas9

INTRODUCTION

Long term clinical benefits of EGFR tyrosine kinase inhibitors (EGFR TKI) in *EGFR* mutant non-small cell lung cancers remain limited by the development of drug resistance [1]. The most common mechanism of resistance to first and second generation EGFR TKIs, the EGFR T790M mutation (60%), can be targeted successfully with third generation drugs such as osimertinib [2]. Recently, osimertinib has been approved as first line therapy for *EGFR* mutant lung cancer [3]. As expected, disease progression due to acquired resistance to osimertinib has emerged, with the most common alteration described to date being the *EGFR* C797S mutation [4]. Activation of parallel signaling pathways (amplification of *HER2* and *MET*) or of downstream signaling (mutations in *KRAS*, *PIK3CA*, and *BRAF*) has also been shown to induce resistance to osimertinib and other EGFR TKIs [5]. Several acquired gene rearrangements, including fusions involving *ALK*, *BRAF*, *FGFR3*, *NTRK1* and *RET* have recently been reported as possible mechanisms of resistance to EGFR TKI [6–11]. Clinically, a combination of an EGFR TKI with a drug targeting either *ALK* or *RET*, has been shown to be effective in lung cancer patients with an *EGFR* mutation and the respective gene fusion. However, only *RET* or *FGFR3* fusions have been experimentally proven to confer resistance to EGFR inhibitors in *EGFR*-mutant lung cancers [7, 12, 13].

Activating *BRAF* fusions typically occur at a very low frequency across a wide variety of cancers with the exception of pilocytic astrocytomas [9, 14]. *BRAF* rearrangements are divided into N-terminal deletions (NTD), kinase domain duplications (KDD) and *BRAF* fusions. Overall, *BRAF* alterations are present in 4.4 % NSCLC, and rearrangements

represent 4.3 % of all alterations [10]. Rearrangements retain the *BRAF* kinase domain at the 3' end, while lacking the N-terminal inhibitory domain. Due to the lack of the N-terminal *BRAF* inhibitory domain, rearrangements result in constitutive dimerization of RAF proteins independently of RAS activation [15], thereby activating downstream MAP kinase signaling.

Here, we report 4 cases of *EGFR* mutant NSCLC with concurrent expression of a *BRAF* fusion and provide functional data supporting *BRAF* fusions as a mechanism of acquired resistance to EGFR therapy in *EGFR* mutant lung adenocarcinomas. In addition, we present data supporting treatment strategies focusing on targeting RAF with pan-RAF inhibitors.

METHODS

Generation of *AGK/BRAF* fusion using CRISPR/Cas9 in *EGFR* mutant lung cancer cell lines

gRNA design and cloning.—In order to faithfully model a *BRAF* fusion, gRNAs were designed to generate a fusion linking *AGK* exons 1–2 with *BRAF* exons 8 – 18. Specifically, four guide RNAs (gRNAs) were designed (Supplemental table 1) to target the intron between *AGK* exons 2 and 3 or *BRAF* exons 7 and 8 and selected using http://crispr.mit.edu/. The placement of these gRNAs aimed to minimize splicing interference by being positioned at least 50 bp-250 bp from the splice site. gRNA cloning was performed according to previously published protocols [16]. 1 μg px458 (containing Cas9 and GFP cDNAs) was digested with 1 μl FastDigest Bpil, 1 μl fast AP, 2 μl 10× FastDigest buffer diluted in 6 μl water at a final volume of 20 μl at 37°C for 45 min. The resulting DNA was cleaned up with PCR clean up kit to a final concentration of 15–30 ng/μl. 1 μl of each pair of gRNA was then phosphorylated and annealed with 1 μl 10× T4 ligation buffer, 0.5 μl T4 polynucleotide kinase and 6.5 μl RNAse/DNAse-free water to a final volume of 10 μl, in a Biorad C1000 Touch thermocycler for 30 min at 37°C, then decrements in temperature from 95°C to 25°C in 5 min intervals. Annealed gRNAs were ligated into px458 using 50 ng of vector, 1.5 μl of annealed gRNAs (1:100 dilution), 5 μl of quick ligase buffer, 1 μl quick ligase with addition of RNAse/DNAse-free water to a final volume of 10 μl, at room temperature for 30 min. The annealed and ligated plasmids were then transformed using TOP10 chemically competent E. coli. The plasmid DNA was extracted and insertion of gRNAs in px458 was confirmed by Sanger sequencing.

Validation of gRNAs.—To test the efficacy of fusion generation, human bronchoepithelial cells (HBEC) (plated at a density of 500,000 cells/well in 6-well plates) were transfected with each possible pair of gRNAs with 1 μg of each CRISPR/Ca9 construct. After 48 h, GFP was readily visible, and after 72 h each pool of cells was harvested for RNA extraction, cDNA synthesis and RT-PCR to detect the fusion mRNA. The pool of cells containing *BRAF* gRNA #4 and AGK gRNA #4 generated detectable fusion mRNA. This pairing (*BRAF* gRNA #4 and *AGK* gRNA #4) was transfected into H1975, HCC827 and PC9 cells plated at a density of 1,500,000 cells/10 cm dish with 7.5 μg of each plasmid and fusion mRNA detected as described above.

Clonal selection.—Transfected cells were maintained in growth media supplemented with 0.5 μM osimertinib to select for a drug-resistant population. The resistant cells were

then replated at a density of 500 cells/10 cm dish to isolate single-cell clones. Colonies were then picked with cloning discs and replated in a 96-well plate for expansion in RPMI containing 10% FBS, 1% antibiotic/antimycotic and 0.5 μM osimertinib. Once clones began to proliferate readily, cells were serially moved to larger containers and then subjected to RT-PCR for fusion detection.

Generation of *BRAF* fusion constructs.—The cDNA encoding *PJA2/BRAF* fusion was amplified from MSK-LX138cl cells by PCR and cloned into pENTR/TOPO vector. The cDNA encoding *AGK/BRAF* fusion was generated by first amplifying the *AGK* and *BRAF* fragments from HEK-293T cells and then assembling the two pieces into Kpn I -EcoRV-digested pENTR1A vector by Gibson assembly. These *BRAF* fusion cDNAs were then subcloned into pLX303 lentiviral transfer vector. The primer sequences used for plasmid construction are shown in Supplemental Table 2. All constructs were confirmed by DNA sequencing. Lentiviruses harboring the two fusions were generated using HEK-293T cells and then used to infect cells the lung cancer lines. Cells stably expressing the cDNAs were selected with blasticidin (20 μg/mL) for 10 days.

shRNA infection and *BRAF* knockdown.—shRNAs (TRCN0000195066 – Sh2, TRCN0000195609 – Sh3 and TRCN0000196844 – Sh1) were obtained from Sigma-Aldrich (St. Louis, MO). Lentiviruses were generated using HEK-293T cells and were used to infect cells. Cells were plated in 6-well plates at a density of 150,000–500,000 cells/well and then infected 24 h later with viral supernatant (MOI=7) expressing *BRAF* shRNAs or non-targeting sequence, mixed with 10 μg/mL polybrene. Infected cells were selected with 5–10 μg/mL puromycin then replated for viability testing with osimertinib or used to detect *BRAF* by RT-qPCR.

RESULTS

Co-expression of *EGFR* mutation and *BRAF* fusions in lung cancer samples refractory to EGFR TKI.

We performed targeted large panel sequencing using the MSK-IMPACT assay [14, 17] on 374 consecutive patients with metastatic *EGFR* mutant lung cancers, including 200 tested prior to receiving an EGFR TKI, 136 tested after progression on an EGFR TKI, and 38 patients with both types of samples. We identified four patients (4/174; 2.3%) with disease progression on EGFR TKI (two on erlotinib; two on erlotinib, followed by osimertinib) with an *EGFR* mutation and a *BRAF* fusion (3 *AGK/BRAF* and 1 *PJA2/BRAF*). In one patient for which paired pre- and post TKI samples were available, an *AGK/BRAF* fusion was present only after progression on erlotinib supporting the hypothesis that *BRAF* fusions are possible acquired mechanisms of drug resistance. The other 3 EGFR TKI-resistant patient samples lacked pre-EGFR TKI data from the same site sample, however one patient had pre-EGFR TKI MSK-IMPACT testing on a lung biopsy and a *BRAF* fusion on a pleural effusion (Supplemental table 5). Importantly, none of 200 patients whose tumor sample was obtained prior to EGFR TKI treatment showed a concurrent *BRAF* fusion.

Clinical course of two patients with matched pre- and post-TKI samples

Case 1.—A 48-year-old man, never smoker, presented with a right cranial nerve 12 palsy and was found to have metastatic lung adenocarcinoma to the brain, liver, bone, and lymphangitic spread in the lungs (patient 2, Supplemental table 4) (Figure 1). Evaluation of the right upper lobe biopsy sample by PCR revealed a 15-base pair *EGFR* exon 19 deletion. The patient received whole brain radiation therapy followed by single agent erlotinib 150 mg daily. A complete depiction of the treatment course and diagnosis is shown in Figure 1A. The patient initially had a robust clinical and radiologic response but after 7.7 months of treatment was noted to have progressive disease in the bone and subsequently liver. A biopsy was performed on the liver and MSK-IMPACT [17] testing revealed a newly acquired *EGFR* T790M mutation. The patient was subsequently given osimertinib 80 mg daily with initial response. After 9.5 months the patient had radiologic and clinical progression with right-sided chest pain and a pleural effusion. A thoracentesis was done with MSK-IMPACT testing revealing a *BRAF* structural rearrangement. Targeted RNAseq using MSK-Fusion Solid, a panel assay based on anchored multiplex PCR [18], was performed and showed the *AGK*/*BRAF* fusion (Supplemental Table 5). The patient was changed to nivolumab but showed further clinical deterioration and died 2 weeks later (Figure 1).

Case 2.—A 69-year-old woman, former smoker (22 pack-years) was diagnosed initially with stage IIa (pT2aN1M0) lung adenocarcinoma status post a left upper lobe lobectomy and mediastinal node dissection followed by adjuvant cisplatin and pemetrexed for 4 cycles (patient 4, Supplemental table 4) (Figure 1). She was maintained on active surveillance for 2.9 years at which time she was noted to have a metastatic recurrence to the brain. She underwent a metastasectomy with pathology of a right frontal lobe metastasis showing a 1.8 cm tumor with predictive immunohistochemistry negative for *EGFR* L858R and *ALK*. MSK-IMPACT analysis revealed an *EGFR* exon 19 deletion. A timeline of the clinical course is shown in Figure 1B. An interval CT scan found enlarging mediastinal lymph nodes and the patient was given erlotinib 150 mg daily. The patient had a clinical and radiologic response to erlotinib, remaining on it for 1.5 years at which point she was noted to have progression in her mediastinal lymph nodes. MSK-IMPACT analysis of the post-erlotinib treatment sample identified the original *EGFR* exon 19 deletion as well as a new *AGK*/*BRAF* fusion (Supplemental Table 5). She was placed on multiple lines of cytotoxic chemotherapy, however, she had continued disease progression and died.

Generation of isogenic *EGFR* mutant cell lines with *BRAF* fusions.—To examine the influence that acquired *BRAF* rearrangements have on sensitivity to EGFR TKIs, we inserted an *AGK/BRAF* fusion into *EGFR* mutant lung cancer cell lines H1975 (T790M, L858R), HCC827 (*EGFR* Ex19del) and PC9 (*EGFR* Ex19del) using CRISPR/Cas9 genome editing [16, 19]. An outline of the experimental scheme is illustrated in Figure 2A. Guides were designed to target intron 1 of *AGK* and intron 7 of *BRAF* in order to generate a fusion of *AGK* exon 2 with exon 8 of *BRAF* (Figure 2A) and cloned into pX458 expression plasmid. Plasmids were introduced and cells selected with osimertinib as described in Methods. All osimertinib-resistant clones were positive for the *AGK/BRAF* fusion by PCR (22 H1975, 16 HCC827 and 20 PC9). Two clones of each cell line that was positive for *AGK/BRAF* fusion at the mRNA and genomic DNA level were selected for further analysis

(Figure 2B). The fusion junction of the two genes was confirmed by Sanger sequencing (Figure 2C).

Expression of *AGK/BRAF* fusion in *EGFR* mutant cell lines induces resistance to EGFR TKIs.—Western blot analysis with phospho-specific BRAF anti-sera confirmed the presence of the AGK/BRAF chimeric protein at the predicted molecular mass of 50 kDa. All cells expressing the *AGK/BRAF* fusion showed enhanced phosphorylation of MEK1/2 and ERK1/2 (Figure 2D) compared to the parental control cells. Importantly, treatment with osimertinib (0.5 μM) blocked activation of MEK1/2, ERK1/2 and STAT3 in parental cells but not in the *AGK/BRAF*-expressing cells, probably due to EGFR-independent activation of the pathways by the BRAF fusion (Figure 2D).

To confirm that expression of *BRAF* fusions can impede osimertinib efficacy, we assessed viability of *EGFR* mutant cell lines expressing *AGK/BRAF* fusion in dose-response studies. Osimertinib inhibited growth of parental HCC827, H1975 and PC9 with IC_{50} value of 0.001, 0.006 and 0.009 μM, respectively. In contrast, clones expressing AGK/BRAF were approximately 1000-fold less sensitive to osimertinib than the parental lines (Figures 2E and 2F). To provide orthogonal validation of these results obtained with the CRISPR-generated *AGK/BRAF* isogenic lines, we also expressed *AGK/BRAF* and *PJA2/BRAF* fusions using lentiviral plasmids harboring the respective fusion cDNAs in H1975 and PC9 cells (Supplementary figure 1A). As shown in Supplementary Figure 1B, expression of the two *BRAF* fusions in H1975 and PC9 cells resulted in lower sensitivity to osimertinib. To ensure that the resistance to EGFR TKIs was due to expression of *BRAF* fusions, we examined viability in two independent clones (H1975-AGK/BRAF-C8 and HCC827-AGK/BRAF-C1) in which *BRAF* was knocked down with two independent shRNAs targeting kinase domain of *BRAF*. Expression of *BRAF* mRNA was reduced by 98.2–100% by the two shRNAs, compared to cells expressing a non-targeting control shRNA (Figure 2G). HCC827 and H1975 clones expressing the *AGK/BRAF* fusion were resensitized to osimertinib upon treatment with these shRNAs targeting the portion of *BRAF* included in the fusion, confirming that the resistance we observed was due to expression of the fusion (>100 fold decrease in IC_{50} compared to non-targeting control) (Figure 2H). Similar results were obtained in cells expressing *AGK/BRAF* and *PJA2/BRAF* cDNAs (Supplementary figure 1C and 1D). Taken together, these results confirm *BRAF* fusions as resistance mechanism to EGFR TKI.

An EGFR TKI-resistant patient derived cell line with *EGFR Ex19 del* and *PJA2/BRAF*.—We generated a patient derived xenograft (MSK-LX138) and paired cell line (referred to as MSKLX138cl) from tissue isolated from patient 1 after resistance to EGFR TKI emerged. MSK-IMPACT analysis of this tumor sample showed a *PJA2-BRAF* fusion and we confirmed the presence and expression of the fusion at genomic DNA, mRNA and protein level (Figure 3A, 3B, 3C). In agreement with the MSK-IMPACT data, Sanger sequencing of the PCR amplicon indicated a fusion between exon 7 of *PJA2* and exon 11 of *BRAF* (Figure 3B), and *EGFR* exon 19 deletion (Supplementary figure 2A). Similar to the observations in the isogenic lung cancer cell lines with *AGK/BRAF* fusion that we generated, MSK-LX138cl cells exhibited high levels of MEK and ERK phosphorylation,

which persisted despite osimertinib treatment. Interestingly, this cell line exhibited no AKT phosphorylation (Figure 3C), suggesting that *BRAF* fusions can drive growth and survival signals independently of the PI3K-AKT pathway. Growth of MSK-LX138cl cells was insensitive to EGFR TKIs (afatinib, erlotinib, osimertinib, gefitinib) and several BRAF inhibitors (vemurafenib, dabrafenib, sorafenib, RXDX-105) (Figure 3D–E). Similar results with BRAF inhibitors were obtained in the established CRISPR fusion clones (Figure 4A). As *BRAF* fusions function as dimers, the lack of activity of vemurafenib and dabrafenib was not unexpected. In agreement with the reduced sensitivity of these cells to EGFR and BRAF inhibitors, there was no apoptosis-related induction in caspase 3/7 activity in response to treatment with several EGFR and RAS-MAPK pathway inhibitors as single agents (osimertinib, erlotinib, trametinib, RXDX-105, sorafenib, dabrafenib) further supporting the resistant nature of this cell line (Figure 3F).

Combined inhibition of MEK and EGFR as potential therapy.—Given the presence of two actionable oncogenes in our cell lines and patients, we tested the hypothesis that co-inhibition of MEK and EGFR could be an efficient therapeutic strategy. Treatment with trametinib alone decreased growth of all cell lines with *EGFR* mutation alone, or with a *BRAF* fusion; cell lines with the *BRAF* fusion were more sensitive, consistent with published data showing only limited activity of MEK inhibitors in *EGFR*-mutated cell lines [20]. Indeed, we found that only a maximum inhibition of 50% cell growth was achieved by trametinib (results not shown). This may indicate that a subpopulation of cells from lines expressing a *BRAF* fusion can still survive after MEK inhibition. Taken together, these support the notion that MEK inhibition alone is not sufficient to fully inhibit growth of *BRAF*-fusion positive cell lines. To determine the combinatorial effect of osimertinib and trametinib we employed the method of Chou-Talalay that was developed to identify if two or more agents act in a synergistic manner [21]. We calculated the combination index (CI) of multiple combinations of different drug concentrations, where CI<1 represents synergy, CI=1 represents an additive effect and CI>1 represents an antagonistic effect, to determine if the two agents can act synergistically. The experiment was performed in MSK-LX138cl (Figure 4B) as well as two of our isogenic *EGFR* mutant cell lines with *AGK/BRAF* fusion (H1975-C1, HCC827-C1). Our results show that trametinib and osimertinib acted in a synergistic manner to inhibit growth up to a concentration of 100 nM.

LY3009120, a pan-RAF inhibitor is effective as a single agent in *BRAF*-fusion-positive cell lines.—*BRAF* rearrangements are grossly insensitive to BRAF inhibitors (eg vemurafenib, dabrafenib) due to homo- and heterodimerization with other RAF proteins [22, 23]. We also show above, as previously described [24], that BRAF inhibitors are not effective in cell lines with *BRAF* fusions. However, RAF inhibitors such as BGB659 and LY3009120 are expected to be effective against the fusions because they can bind and inhibit all RAF isoforms [25–29]. Treatment of MSK-LX138cl with LY3009120 resulted in complete inhibition of growth with IC_{50} = 0.006 μM (Figure 5A). The melanoma cell line A375, which harbors a *BRAF* V600E mutation [30], was used as a positive control in these experiments. We next examined the effect of LY3009120 on caspase 3/7 activity. LY3009120 caused a small but significant increase in caspase 3/7 activity, similar to that observed with trametinib+osimertinib in MSK-LX138cl (Figure 4F) and HCC827-AGK/

BRAF-C1 cells, but not in the parental HCC827 cell line (Figure 5C). Finally, to better understand how LY3009120 inhibits growth, we examined its effect on phosphorylation of BRAF fusion and other downstream signaling proteins. LY3009120 at 0.1 μM caused a profound reduction in phosphorylation of MEK, ERK and STAT3 (Figure 5B).

DISCUSSION

The present study establishes *BRAF* fusions as a mechanism of resistance to EGFR TKI in *EGFR*-mutant NSCLC and offers two potential therapeutic strategies to circumvent the drug resistance, namely combined inhibition of MEK and EGFR, or inhibition of BRAF fusion. Of seven patients with *BRAF* fusion present on MSK-IMPACT (n = 374), four had concomitant *EGFR* driver mutations suggesting that the co-occurrence of *EGFR* mutations and *BRAF* fusion is a rare but recurrent event. Importantly, all 4 patients were resistant to EGFR TKIs (erlotinib or osimertinib), and in two of four cases the *BRAF* fusions were confirmed to be acquired because pre-TKI samples were available and negative for *BRAF* fusion. *AGK*, which, like *BRAF*, resides at 7q34, encodes a mitochondrial membrane protein involved in lipid and glycerolipid metabolism, whereas PJA2 protein (encoded by a gene at 5q21) has E2-dependent E3 ubiquitin-protein ligase activity. *AGK/BRAF* fusions have been described in melanomas, gliomas, and cancers of the lung, thyroid, and breast [14]. To the best of our knowledge, this is the first report of a *PJA2/BRAF* fusion. Multiple cellular models including one patient-derived cell line and isogenic *EGFR*-mutated lung cancer cell line models demonstrated that expression of *BRAF* fusion mediated resistance to EGFR TKIs. In these models, we observed activation of the MEK-ERK pathway independently of *EGFR*. We further found that loss of *BRAF* fusion expression restores sensitivity to EGFR TKI. Taken together these results indicate that *BRAF* fusions drive resistance to EGFR TKIs in a subset of *EGFR* mutant NSCLC and provides a pathway for developing a viable therapeutic strategy.

It is customary to express a cDNA for a given gene either by lipid-based transfection or viral transduction to determine if expression of the gene alters biological properties such as response to small molecules. These methods of gene expression typically result in supraphysiologic levels of the protein because multiple copies of the cDNA are usually introduced, and expression is driven from a strong, constitutively active viral promoter. Therefore, there is often a concern that the observed results may be an artifact of overexpression of the protein. To avoid this pitfall, we engineered the *AGK/BRAF* fusion using CRISPR-Cas9-mediated genome editing in lung cancer cells harboring drug-sensitive *EGFR* mutations. The advantage of this method over conventional exogenous cDNA expression is that the *BRAF* fusion is expressed from the endogenous, non-amplified allele, resulting in a physiological level of protein expression. Using this approach, we demonstrated that a physiological level of *AGK/BRAF* fusion was able to induce resistance to EGFR inhibitors in *EGFR*-mutant lung cancer cell lines. These results were concordant with data obtained by overexpression of *BRAF* fusions using lentiviral vectors harboring the respective cDNAs. Our approach represents a methodological advance that can be used to model other fusion genes as mechanisms of resistance.

Although *BRAF* fusion may seem to be an obvious therapeutic target, FDA-approved BRAF inhibitors have not been effective against *BRAF* fusions [24, 31–33] and have not always been effective against *BRAF* mutants. As previously described, *BRAF* V600E-positive colorectal cancers have notoriously been insensitive to selective BRAF inhibitors (vemurafenib or dabrafenib), due to feedback activation of EGFR and subsequent RAF dimerization [34]. A similar resistance mechanism has been noted in *BRAF* V600E melanomas, where RAF inhibition abrogates ERK activation, which then terminates the high ERK negative feedback on RTK-dependent activation of RAS, leading to consequent RAF dimerization and ERK reactivation [35]. This ineffectiveness of FDA-approved BRAF drugs against *BRAF* fusions is highlighted by the fact that an *AGAP3/BRAF* fusion has been proposed as a mechanism of acquired resistance to vemurafenib in *BRAF* V600E melanoma [24]. When compounds like vemurafenib and dabrafenib bind to the first site within the BRAF dimer, affinity for the second dimer site is significantly lower, explaining why traditional BRAF inhibitors do not abrogate ERK phosphorylation in *BRAF* fusion-positive tumors [36]. BRAF V600E mutants can become resistant to BRAF inhibitors via formation of BRAF dimers by the mechanism described above [23, 37], which prompted development of pan-RAF inhibitors [26, 38]. Yao et al have reported superiority of a dual RAF inhibitor BGB659 over BRAF inhibitors [36]. Similarly, Peng et al reported the development of LY3009120, a pan-RAF inhibitor that binds simultaneously to two sites of BRAF dimers and equally inhibits all RAF isoforms (ARAF, BRAF, CRAF) with similar affinity [25–29]. We found LY3009120 to be very active against cell lines with *BRAF* fusions as a single agent. Taken together, this indicates that pan-RAF inhibition is a superior single agent strategy for targeting these acquired *BRAF* fusions. Notably, we (N.X.R.) have recently shown that another promising RAF inhibitor, PLX8394, selectively disrupts BRAF dimers, sparing CRAF homodimer-dependent RAF function in normal cells, which may lead to a better safety profile clinically [39]. Clinical studies will be needed to determine if RAF inhibitors are effective against tumors with *BRAF* fusions as a single agent or should be combined with an EGFR TKI to maximize the effectiveness.

To identify potential therapeutic strategies for patients with co-expression of *EGFR* mutant and *BRAF* fusion that can be utilized immediately, we investigated the effectiveness of a combination of trametinib and osimertinib. We found that combined inhibition of MEK and EGFR with these drugs inhibited growth of isogenic cell line models as well as a patient-derived cell line with a *BRAF* fusion and *EGFR* mutation (established from a patient who did not respond to EGFR drugs) in a synergistic manner. The maximum inhibition of growth that we observed was 76%, which may have been due to reactivation of HER2 and ERK following the prolonged treatment of cells with osimertinib and trametinib, respectively (data not shown). Nevertheless, these results suggest that combined MEK and EGFR inhibition is a possible treatment strategy in the absence of more effective FDA-approved RAF inhibitors that are effective against *BRAF* fusions.

Supplementary Material

Refer to Web version on PubMed Central for supplementary material.

ACKNOWLEDGEMENTS:

This work was supported by NIH grants P01 CA129243, P30 CA008748, and U54 OD020355. The authors are grateful to Igor Odintsov and Dr. Zebing Liu for critical reading of the manuscript and helpful suggestions during the course of this study, respectively.

REFERENCES:

1. Stewart EL, et al., Known and putative mechanisms of resistance to EGFR targeted therapies in NSCLC patients with EGFR mutations-a review. Transl Lung Cancer Res, 2015 4(1): p. 67–81. [PubMed: 25806347]
2. Goss G, et al., Osimertinib for pretreated EGFR Thr790Met-positive advanced non-small-cell lung cancer (AURA2): a multicentre, open-label, single-arm, phase 2 study. Lancet Oncol, 2016 17(12): p. 1643–1652. [PubMed: 27751847]
3. Soria JC, et al., Osimertinib in Untreated EGFR-Mutated Advanced Non-Small-Cell Lung Cancer. N Engl J Med, 2018 378(2): p. 113–125. [PubMed: 29151359]
4. Thress KS, et al., Acquired EGFR C797S mutation mediates resistance to AZD9291 in non-small cell lung cancer harboring EGFR T790M. Nat Med, 2015 21(6): p. 560–2. [PubMed: 25939061]
5. Ho C-C, et al., Acquired BRAF V600E Mutation as Resistant Mechanism after Treatment with Osimertinib. Journal of Thoracic Oncology, 2017 12(3): p. 567–572. [PubMed: 27923714]
6. Ou S, et al., MA 12.03 Kinase Fusions as Recurrent Mechanisms of Acquired Resistance in EGFR-Mutated Non-Small Cell Lung Cancer (NSCLC). Journal of Thoracic Oncology, 2017 12(11): p. S1848.
7. Offin M, et al., Acquired ALK and RET Gene Fusions as Mechanisms of Resistance to Osimertinib in EGFR-Mutant Lung Cancers. JCO Precision Oncology, 2018(2): p. 1–12.
8. Klempner SJ, et al., Emergence of RET rearrangement co-existing with activated EGFR mutation in EGFR-mutated NSCLC patients who had progressed on first- or second-generation EGFR TKI. Lung Cancer, 2015 89(3): p. 357–359. [PubMed: 26187428]
9. Ross JS, et al., The distribution of BRAF gene fusions in solid tumors and response to targeted therapy. Int J Cancer, 2016 138(4): p. 881–90. [PubMed: 26314551]
10. Sheikine Y, et al., BRAF in Lung Cancers: Analysis of Patient Cases Reveals Recurrent BRAF Mutations, Fusions, Kinase Duplications, and Concurrent Alterations. JCO Precision Oncology, 2018(2): p. 1–15. [PubMed: 30949620]
11. Schrock AB, et al., Receptor Tyrosine Kinase Fusions and BRAF Kinase Fusions are Rare but Actionable Resistance Mechanisms to EGFR Tyrosine Kinase Inhibitors. J Thorac Oncol, 2018 13(9): p. 1312–1323. [PubMed: 29883838]
12. Piotrowska Z, et al., Landscape of acquired resistance to osimertinib in EGFR-mutant NSCLC and clinical validation of combined EGFR and RET inhibition with osimertinib and BLU-667 for acquired RET fusion. Cancer Discov, 2018.
13. Ou SI, et al., Emergence of FGFR3-TACC3 fusions as a potential by-pass resistance mechanism to EGFR tyrosine kinase inhibitors in EGFR mutated NSCLC patients. Lung Cancer, 2017 111: p. 61–64. [PubMed: 28838400]
14. Zehir A, et al., Mutational landscape of metastatic cancer revealed from prospective clinical sequencing of 10,000 patients. Nat Med, 2017 23(6): p. 703–713. [PubMed: 28481359]
15. Kim HS, et al., Oncogenic BRAF fusions in mucosal melanomas activate the MAPK pathway and are sensitive to MEK/PI3K inhibition or MEK/CDK4/6 inhibition. Oncogene, 2017 36(23): p. 3334–3345. [PubMed: 28092667]
16. Ran FA, et al., Genome engineering using the CRISPR-Cas9 system. Nat Protoc, 2013 8(11): p. 2281–2308. [PubMed: 24157548]
17. Cheng DT, et al., Memorial Sloan Kettering-Integrated Mutation Profiling of Actionable Cancer Targets (MSK-IMPACT): A Hybridization Capture-Based Next-Generation Sequencing Clinical Assay for Solid Tumor Molecular Oncology. J Mol Diagn, 2015 17(3): p. 251–64. [PubMed: 25801821]

18. Zheng Z, et al., Anchored multiplex PCR for targeted next-generation sequencing. Nat Med, 2014 20(12): p. 1479–84. [PubMed: 25384085]
19. Spraggon L, et al., Generation of conditional oncogenic chromosomal translocations using CRISPR-Cas9 genomic editing and homology-directed repair. J Pathol, 2017 242(1): p. 102–112. [PubMed: 28188619]
20. Chiba M, et al., MEK inhibitors against MET-amplified non-small cell lung cancer. Int J Oncol, 2016 49(6): p. 2236–2244. [PubMed: 27748834]
21. Chou TC and Talalay P, Quantitative analysis of dose-effect relationships: the combined effects of multiple drugs or enzyme inhibitors. Adv Enzyme Regul, 1984 22: p. 27–55. [PubMed: 6382953]
22. Sievert AJ, et al., Paradoxical activation and RAF inhibitor resistance of BRAF protein kinase fusions characterizing pediatric astrocytomas. Proc Natl Acad Sci U S A, 2013 110(15): p. 5957–62. [PubMed: 23533272]
23. Poulikakos PI, et al., RAF inhibitor resistance is mediated by dimerization of aberrantly spliced BRAF(V600E). Nature, 2011 480(7377): p. 387–90. [PubMed: 22113612]
24. Kulkarni A, et al., BRAF Fusion as a Novel Mechanism of Acquired Resistance to Vemurafenib in BRAF(V600E) Mutant Melanoma. Clin Cancer Res, 2017 23(18): p. 5631–5638. [PubMed: 28539463]
25. Peng SB, et al., Inhibition of RAF Isoforms and Active Dimers by LY3009120 Leads to Anti-tumor Activities in RAS or BRAF Mutant Cancers. Cancer Cell, 2015 28(3): p. 384–98. [PubMed: 26343583]
26. Vakana E, et al., LY3009120, a panRAF inhibitor, has significant anti-tumor activity in BRAF and KRAS mutant preclinical models of colorectal cancer. Oncotarget, 2017 8(6): p. 9251–9266. [PubMed: 27999210]
27. Yao YM, et al., Mouse PDX Trial Suggests Synergy of Concurrent Inhibition of RAF and EGFR in Colorectal Cancer with BRAF or KRAS Mutations. Clin Cancer Res, 2017 23(18): p. 5547–5560. [PubMed: 28611205]
28. Wei WJ, et al., Obatoclax and LY3009120 Efficiently Overcome Vemurafenib Resistance in Differentiated Thyroid Cancer. Theranostics, 2017 7(4): p. 987–1001. [PubMed: 28382170]
29. Jain P, et al., CRAF gene fusions in pediatric low-grade gliomas define a distinct drug response based on dimerization profiles. Oncogene, 2017 36(45): p. 6348–6358. [PubMed: 28806393]
30. Giard DJ, et al., In vitro cultivation of human tumors: establishment of cell lines derived from a series of solid tumors. J Natl Cancer Inst, 1973 51(5): p. 1417–23. [PubMed: 4357758]
31. Corcoran RB, et al., EGFR-mediated re-activation of MAPK signaling contributes to insensitivity of BRAF mutant colorectal cancers to RAF inhibition with vemurafenib. Cancer Discov, 2012 2(3): p. 227–35. [PubMed: 22448344]
32. Montagut C and Settleman J, Targeting the RAF-MEK-ERK pathway in cancer therapy. Cancer Lett, 2009 283(2): p. 125–34. [PubMed: 19217204]
33. Holderfield M, et al., Targeting RAF kinases for cancer therapy: BRAF-mutated melanoma and beyond. Nat Rev Cancer, 2014 14(7): p. 455–67. [PubMed: 24957944]
34. Prahallad A, et al., Unresponsiveness of colon cancer to BRAF(V600E) inhibition through feedback activation of EGFR. Nature, 2012 483(7387): p. 100–3. [PubMed: 22281684]
35. Lito P, et al., Relief of profound feedback inhibition of mitogenic signaling by RAF inhibitors attenuates their activity in BRAFV600E melanomas. Cancer Cell, 2012 22(5): p. 668–82. [PubMed: 23153539]
36. Yao Z, et al., BRAF Mutants Evade ERK-Dependent Feedback by Different Mechanisms that Determine Their Sensitivity to Pharmacologic Inhibition. Cancer Cell, 2015 28(3): p. 370–83. [PubMed: 26343582]
37. Poulikakos PI, et al., RAF inhibitors transactivate RAF dimers and ERK signalling in cells with wild-type BRAF. Nature, 2010 464(7287): p. 427–30. [PubMed: 20179705]
38. Henry JR, et al., Discovery of 1-(3,3-dimethylbutyl)-3-(2-fluoro-4-methyl-5-(7-methyl-2-(methylamino)pyrido[2,3-d]pyrimidin-6-yl)phenyl)urea (LY3009120) as a pan-RAF inhibitor with minimal paradoxical activation and activity against BRAF or RAS mutant tumor cells. J Med Chem, 2015 58(10): p. 4165–79. [PubMed: 25965804]

39. Yao Z, et al., RAF inhibitor PLX8394 selectively disrupts BRAF dimers and RAS-independent BRAF-mutant-driven signaling. Nat Med, 2018.

40. Yang X, et al., A public genome-scale lentiviral expression library of human ORFs. Nat Methods, 2011 8(8): p. 659–61. [PubMed: 21706014]

41. Somwar R, et al., Identification and preliminary characterization of novel small molecules that inhibit growth of human lung adenocarcinoma cells. J Biomol Screen, 2009 14(10): p. 1176–84. [PubMed: 19887599]

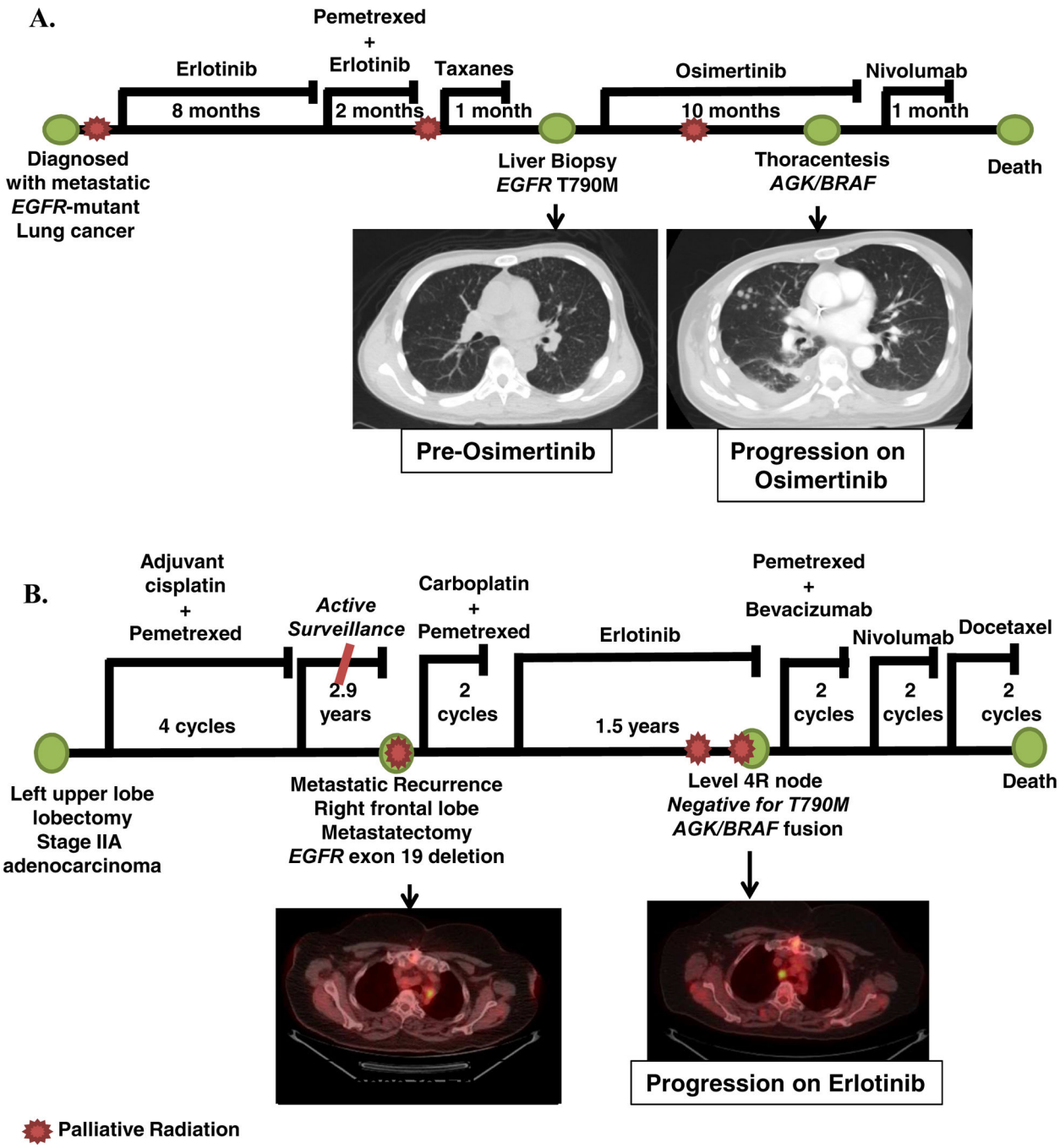

FIGURE 1. Clinical information for patients with resistance to EGFR TKI and *BRAF* fusions.

A. Disease course of patient 2, found to have acquired resistance to osimertinib and *AGK/BRAF* fusion. **B**. Disease course of patient 4, found to have acquired resistance to erlotinib and progressive mediastinal disease with *AGK/BRAF* fusion.

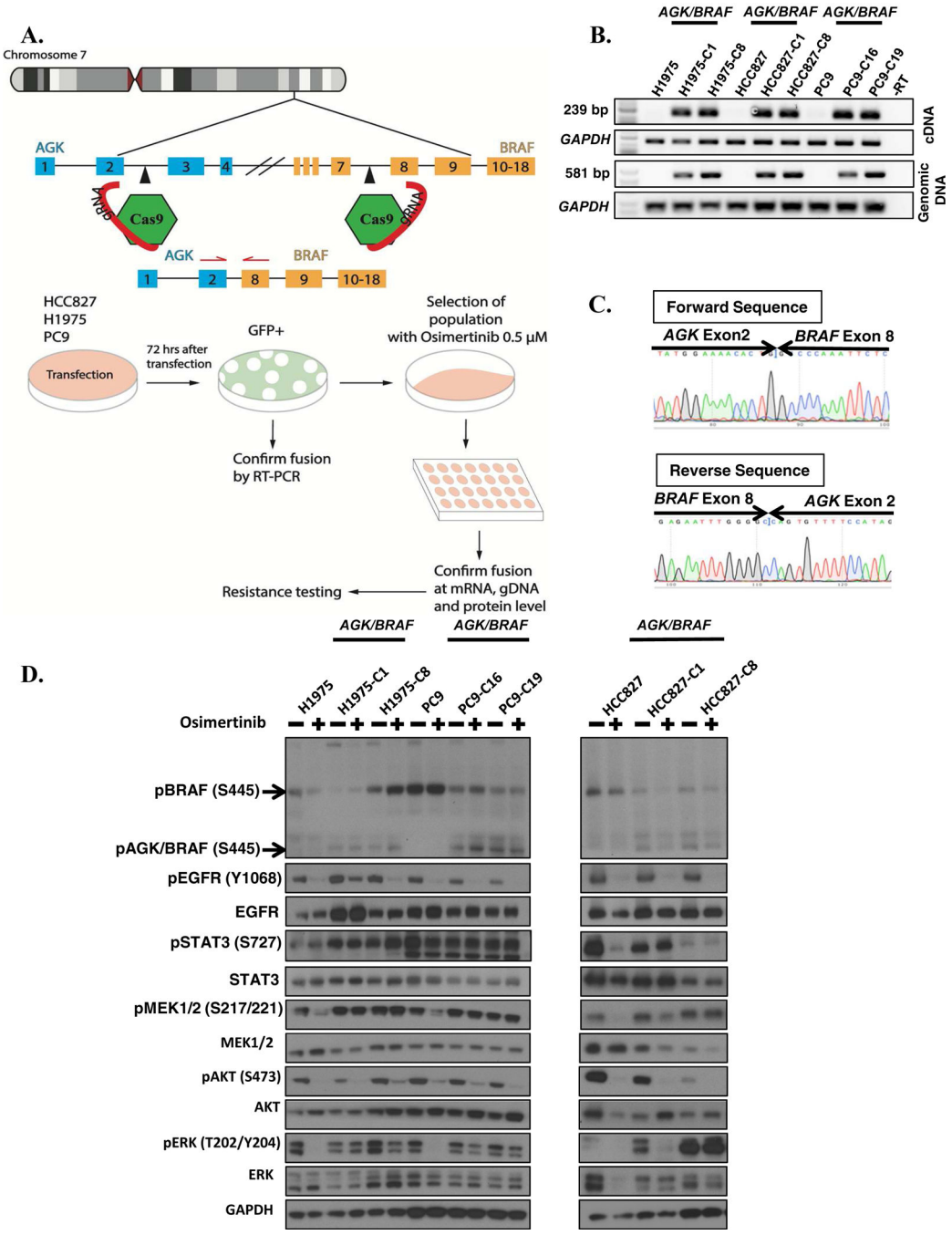

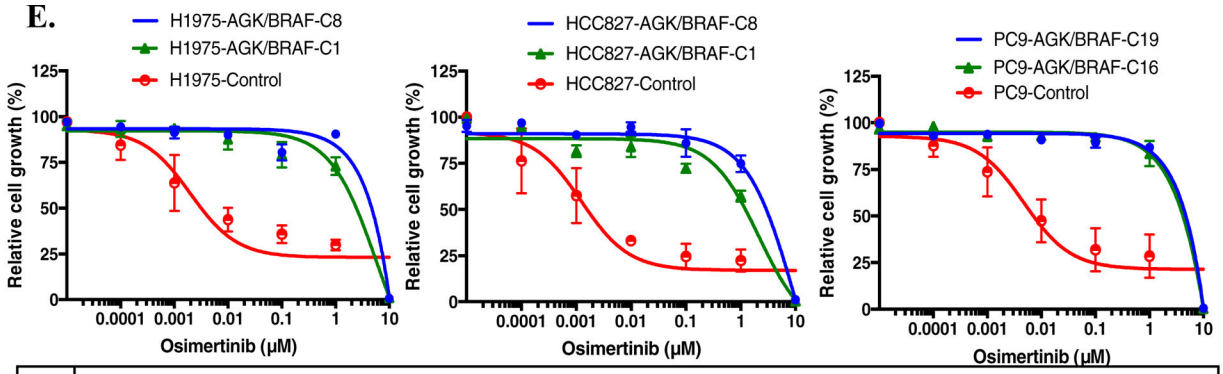

F.

Osimertinib IC_{50} For Inhibition of Growth [μM]								
H1975	H1975-AGK/BRAF-C1	H1975-AGK/BRAF-C8	HCC827	HCC827-AGK/BRAF-C1	HCC827-AGK/BRAF-C8	PC9	PC9-AGK/BRAF-C16	PC9-AGK/BRAF-C19
0.006	1.306	2.566	0.001	1.305	3.235	0.009	2.609	2.612

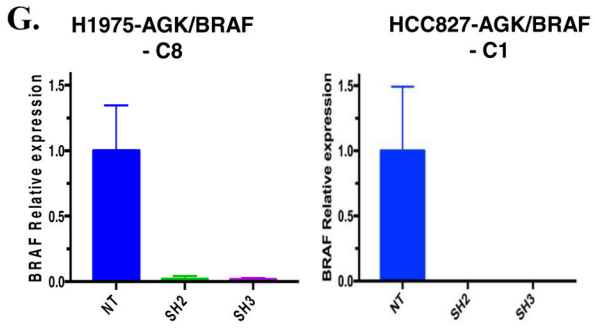

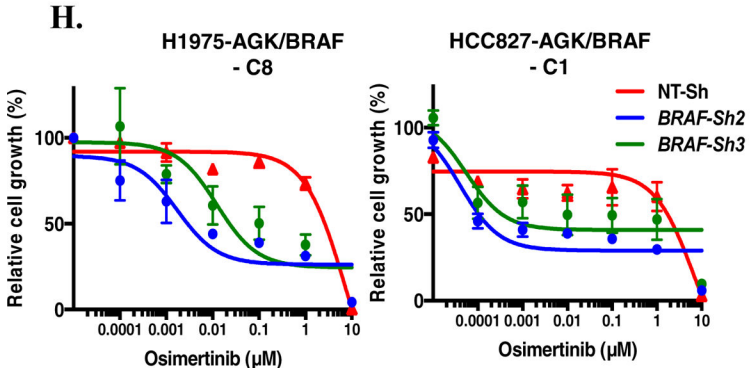

Osimertinib IC_{50} For Inhibition of Growth [μM]					
H1975-AGK/BRAF-C8			HCC827-AGK/BRAF-C1		
NT	BRAF Sh2	BRAF Sh3	NT	BRAF Sh2	BRAF Sh3
7.2	0.002	0.01	6.6	0.0004	0.0005

FIGURE 2. Generation and characterization of CRISPR/Cas9 *AGK/BRAF* cell lines.

A. CRISPR/Cas9 genome engineering protocol scheme. **B**. Expression of *AGK/BRAF*. **C**. Sanger sequencing of PCR product confirming fusion in cell line of *AGK* exon 2 with exon 8 of *BRAF*. **D**. H1975 and PC9 cells expressing *AGK/BRAF* were treated with 0.5 osimertinib for 1 h, whole-cell extracts prepared and then lysates were subjected to immunoblotting. Results represent 3 independent experiments. **E**. The indicated cell lines were plated at a density 7,500/well in 96-well plates, treated with osimertinib for 96 h and the IC_{50} values for growth inhibition are shown in the Table in panel **F**. **G-H**. Cells were

plated at a density of 150,000 cells/well in 6-well plates then infected 24 h later with lentiviruses harboring the indicated shRNAs and then selected with puromycin 48 h later. *BRAF* mRNA levels was determined by qRT-PCR (**G**) or cells were replated in osimertinib and growth assessed 96 later (**H**). IC_{50} values for growth inhibition were determined by nonlinear regression analysis using Graphpad Prism software. Results represent the mean ± SD of 2 experiments.

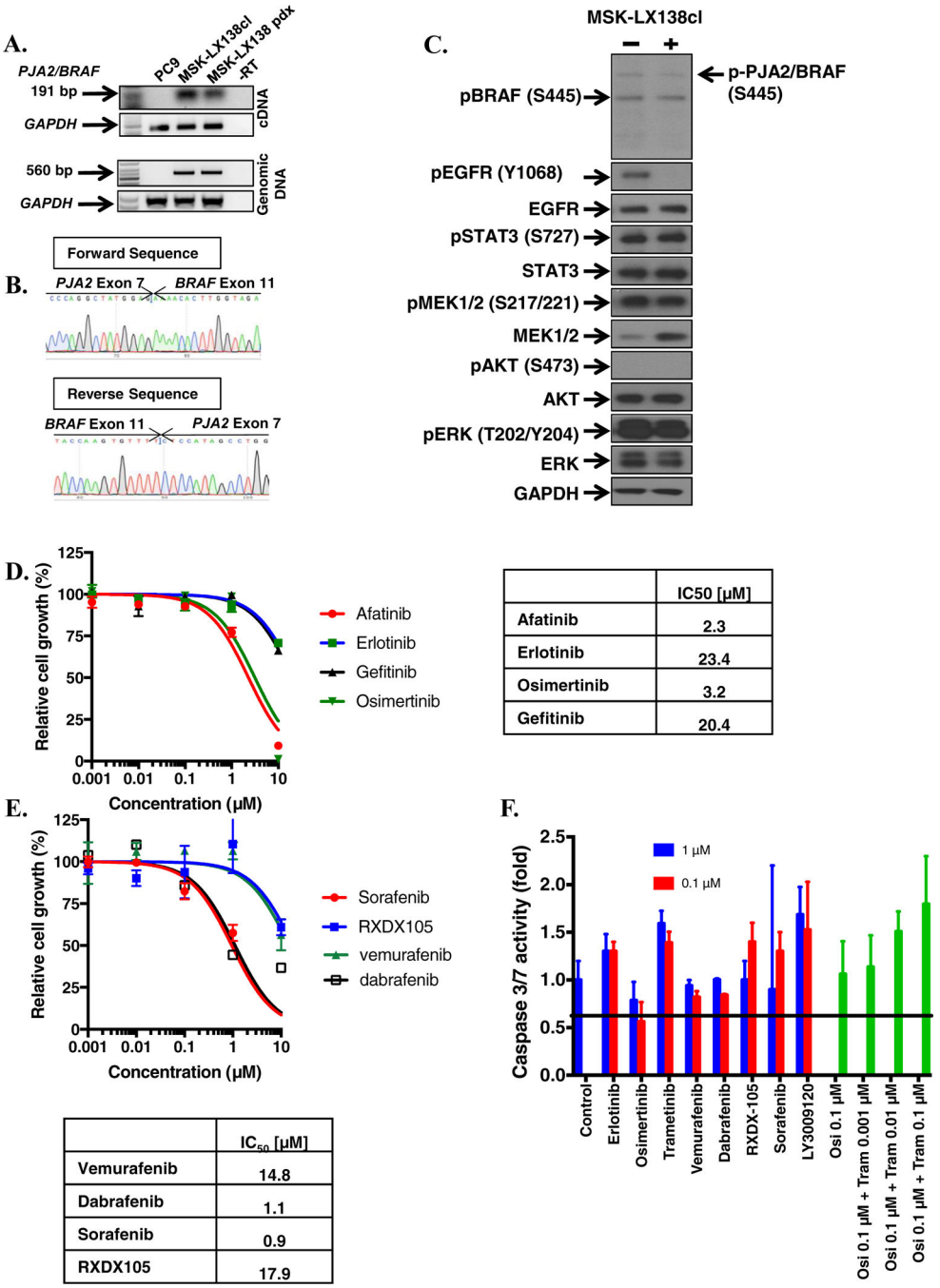

	IC50 [μM]
Afatinib	2.3
Erlotinib	23.4
Osimertinib	3.2
Gefitinib	20.4

	IC_{50} [μM]
Vemurafenib	14.8
Dabrafenib	1.1
Sorafenib	0.9
RXDX105	17.9

FIGURE 3. Characterization of an *EGFR* mutant cell line with *PJA2/BRAF* fusion.

A. Expression of *PJA2/BRAF* in a patient-derived cell line, MSK-LX138cl, and xenograft tissue. **B**. Sanger sequencing of PCR product confirming a fusion between *PJA2* exon 7 and *BRAF* exon 11. **C**. MSK-LX138cl cells were treated with 0.5 osimertinib for 1 h, whole-cell extracts prepared and then lysates were subjected to immunoblotting. Results represent 3 independent experiments. **D-E**. MSK-LX138cl cells were plated at a density 7,500/well in a 96-well plates, treated with EGFR (**D**) or BRAF (**E**) inhibitors. IC_{50} values for growth inhibition were determined by nonlinear regression analysis using Graphpad Prism software.

F. 50,000 MSK-LX138cl cells/well were plated in 96-well plates, the following day they were treated with 0.1 or 1 μM of the indicated agents or a combination of osimertinib, and trametinib. Caspase 3/7 activity was determined 48 h later. Results represent the mean ± SD of 2 experiments.

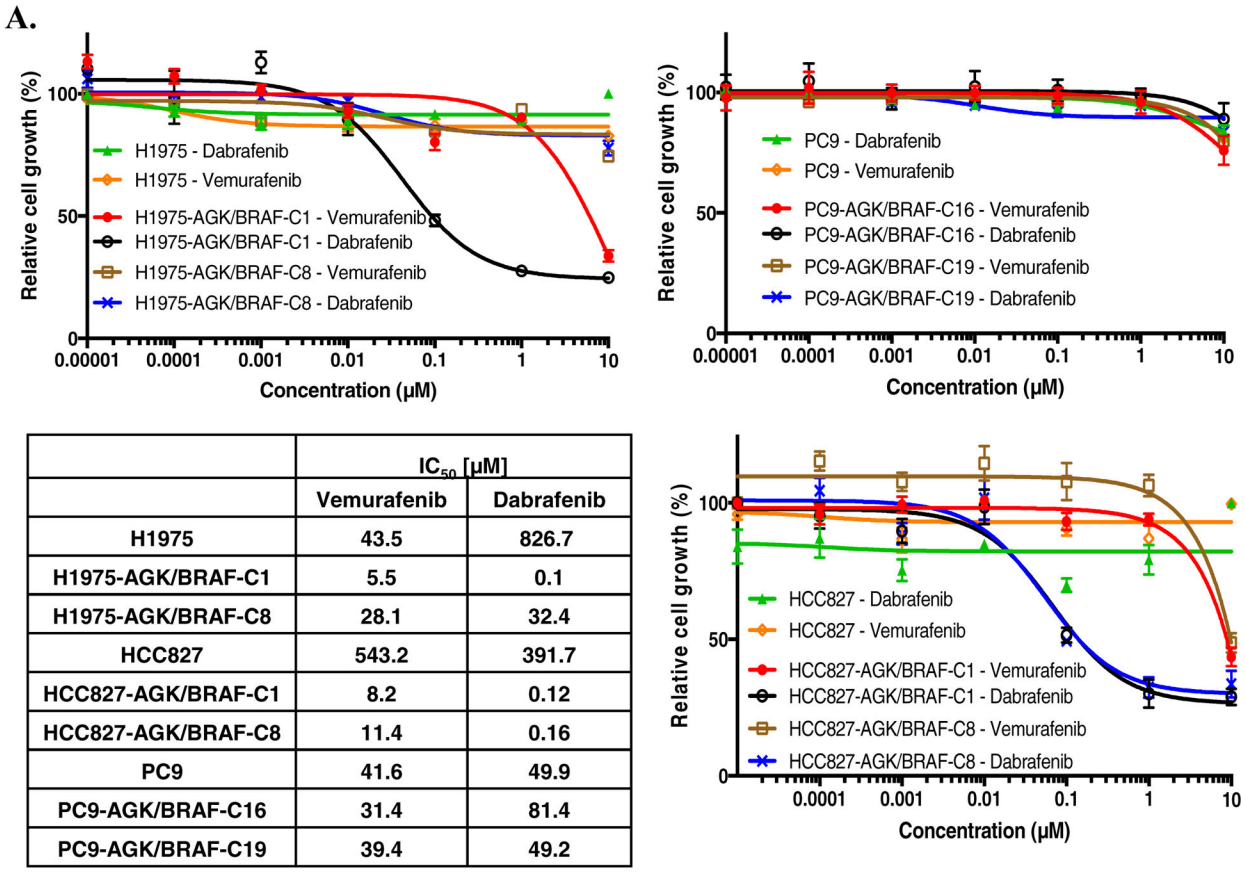

	IC_{50} [μM]	
	Vemurafenib	Dabrafenib
H1975	43.5	826.7
H1975-AGK/BRAF-C1	5.5	0.1
H1975-AGK/BRAF-C8	28.1	32.4
HCC827	543.2	391.7
HCC827-AGK/BRAF-C1	8.2	0.12
HCC827-AGK/BRAF-C8	11.4	0.16
PC9	41.6	49.9
PC9-AGK/BRAF-C16	31.4	81.4
PC9-AGK/BRAF-C19	39.4	49.2

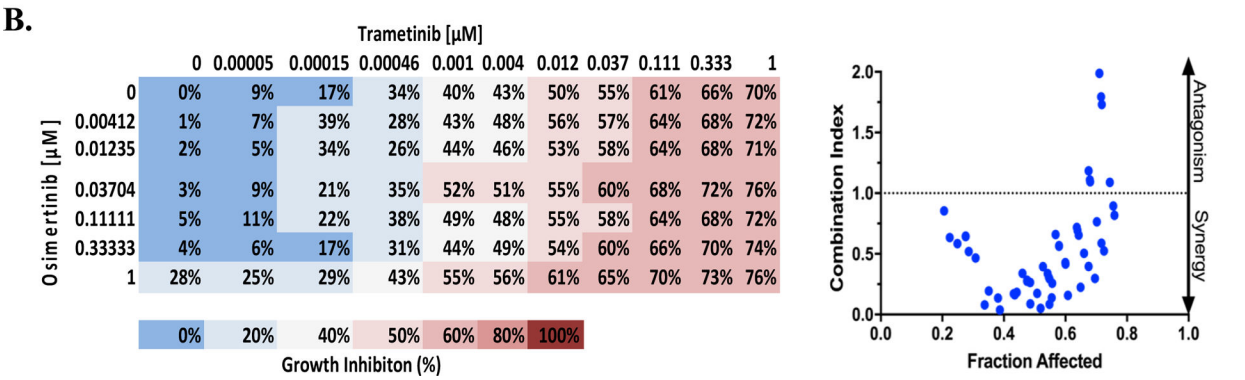

FIGURE 4. Combined inhibition of MEK and EGFR is effective and reducing growth of cells with *EGFR* mutation.

A. Cells were plated at a density of 7,500 cells/well in 96-well plate and treated with vemurafenib or dabrafenib for 96 h then growth was determined. IC_{50} values for growth inhibition are shown **(Right)**. **B**. MSK-LX138cl cells were plated at a density of 7,500 cells/well in 96-well plates and treated with trametinib (0–1μM) and osimertinib (0–1μM) for 96 h. Growth inhibition was then determined and combination index calculated using CompuSyn software. Data represent the mean value of growth inhibition ratio at each

concentration of the drugs in two independent experiments. Dot plot indicates the combination index and fraction affected (inhibition ratio) of various drug concentrations.

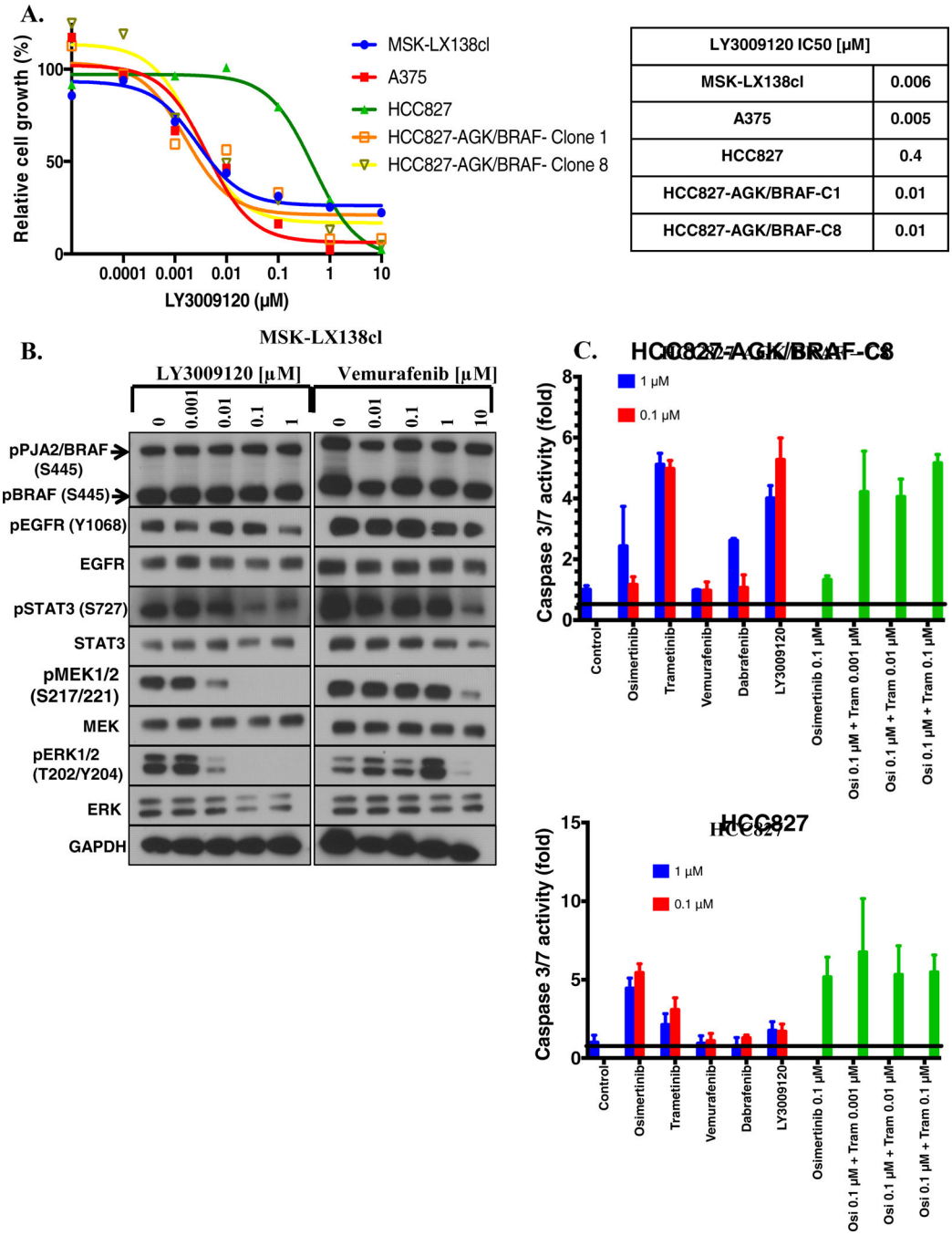

LY3009120 IC50 [μM]	
MSK-LX138cl	0.006
A375	0.005
HCC827	0.4
HCC827-AGK/BRAF-C1	0.01
HCC827-AGK/BRAF-C8	0.01

FIGURE 5. The pan-RAF inhibitor LY3009120 effectively inhibits growth of *EGFR* mutant cell lines with *BRAF* fusions.

A. Cells were plated in 96-well plates, treated with LY3009120 and then growth determined **(Left)**. IC_{50} values for growth inhibition were determined by nonlinear regression analysis using GraphPad Prism software **(Right)**. **B**. MSK-LX138cl cells were treated with the indicated concentration of LY3009120 or vemurafenib for 1 h then whole-cell extracts prepared and immunoblotted for the indicated proteins. Results are representative of two independent experiments. **C**. Cells were treated with 0.1 or 1 μM of the indicated

compounds or osimertinib/trametinib combinations and caspase 3/7 activity determined 48 h later.